Published in final edited form as:
Langmuir. 2010 March 2; 26(5): 3744–3752. doi:10.1021/la903038a.

Dynamics of Liquid Plugs of Buffer and Surfactant Solutions in a Micro-Engineered Pulmonary Airway Model

Hossein Tavana[a], **Chuan-Hsien Kuo**[a], **Qian Yi Lee**[a], **Bobak Mosadegh**[a], **Dongeun Huh**[a], **Paul J. Christensen**[b], **James B. Grotberg**[a], and **Shuichi Takayama**[a,*]

[a] Department of Biomedical Engineering, University of Michigan, 2200 Bonisteel Blvd., Ann Arbor, MI 48109-2099, USA

[b] Department of Internal Medicine, University of Michigan, 1500 East Medical Center Drive, Ann Arbor, MI 48109-2399, USA

Abstract

We describe a bio-inspired microfluidic system that resembles pulmonary airways and enables on-chip generation of airway occluding liquid plugs from a stratified air-liquid two-phase flow. User-defined changes in the air stream pressure facilitated by mechanical components and tuning the wettability of the microchannels enable generation of well-defined liquid plugs. Significant differences are observed in liquid plug generation and propagation when surfactant is added to the buffer. The plug flow patterns suggest a protective role of surfactant for airway epithelial cells against pathological flow-induced mechanical stresses. We discuss the implications of the findings for clinical settings. This approach and the described platform will enable systematic investigation of the effect of different degrees of fluid mechanical stresses on lung injury at the cellular level and administration of exogenous therapeutic surfactants.

Introduction

The airway tree of the lung consists of a branching network of tubes that become shorter, narrower, and more numerous as they penetrate deeper into the lung.[1] The airway is normally lined with a dynamic thin liquid film secreted and maintained by airway epithelial cells. Airways less than 1–2 mm in diameter that include membranous, terminal and respiratory bronchioles as well as alveolar ducts are known as distal airways.[2] Due to their small size, distal airways are prone to closure at low lung volumes,[3] e.g. at the end of expiration. Pulmonary surfactant within the liquid lining film reduces the surface tension at the air-liquid interface of the airways and prevents airway collapse.[4, 5] Abnormalities in biochemical and biophysical properties of surfactant cause instabilities of the air-liquid interface in various respiratory disorders[6–11] creating liquid plugs which obstruct airflow and impede gas exchange.[12] During inflation of the lung, the pressure associated with the inspired air moves the plug downstream. The plug leaves behind a trailing film as it propagates, becomes shorter when the trailing film is thicker than the precursor film,[13] and can eventually rupture re-establishing airflow. This process is known as “airway closure and reopening” and is schematically shown in Fig. 1a. Computational models show that reopening of occluded

*Corresponding Author, Tel.: (734) 615-5539, Fax: (734) 936-1905, takayama@umich.edu.

Supporting Information Available (i) Variation of microfluidic airway pressure due to changes in air and liquid flow rates, (ii) variation of peak differential pressure and plug size with pinch valve closure time, (iii) variation of plug length with peak differential pressure non-dimensionalized with respect to the solid-liquid interfacial tension, (iv) a monolayer of lung epithelial cells, (v) a video of multiple plug formation with PBS, (vi) a video of precursor surfactant film formation on channel walls. This information is available free of charge via the Internet at http://pubs.acs.org/.

airways exerts abnormal fluid mechanical stresses on airway walls that may damage the lining epithelial layer.[13–17]

Liquid plugs may also form during clinical therapies such as mechanical ventilation (MV) and surfactant replacement therapy (SRT).[18–20] MV is used to support gas exchange for patients with a wide range of respiratory disorders. When the disorder is also accompanied by surfactant dysfunction, cyclic liquid plug-mediated closure and subsequent reopening of airways happens that may exacerbate damage to epithelium.[21–23] In SRT that involves administration of exogenous surfactant into patients' lungs through the endotracheal tube, homogeneous surfactant delivery usually requires a fast injection, which in turn results in the formation of a surfactant plug.[5, 24] The plug is then propelled distally into airways during forced inspiration. There is also a great deal of interest in using liquid plugs as vehicles for targeted drug delivery in various lung diseases.

Despite being implicated in a wide range of events in lungs, liquid plugs have not been studied experimentally in detail mainly due to the difficulty of recreating pulmonary airway-associated flows in vitro. Recently, our group developed a microfluidic device consisting of a plug generator and a cell culture chamber.[25] Liquid plugs of phosphate buffered saline (PBS) were generated by switching off and on the air stream of a stratified air-liquid two-phase flow and subsequently propagated over a monolayer of epithelial cells under the air stream pressure. Although useful, this system lacked precise control and measurement of pressure levels making it difficult to relate plug generation and propagation to physiological MV- and SRT-type applications where a fine control over airway pressures is required. Here, we describe an automated microfluidic pulmonary airway model that is integrated with a computer-controlled on-chip plug generator and equipped with pressure sensors, solenoid valves and flow meters to generate and monitor a wide range of airway pressures. This platform enables formation and propagation of liquid plugs of both PBS and, for the first time, surfactant-containing solutions with defined size and speed. Unlike most existing plug generating mechanisms that utilize two-phase flows in different channel configurations (e.g. a T-junction) and result in a "train" of liquid plugs within an air stream,[26, 27] study of liquid plug dynamics in lung airway models requires the flexibility of user-defined timing of formation and propagation of individual plugs.[28] The platform described here facilitates such fundamental investigations. Our analysis shows that channel surface wettability, air pressure, and fluid properties determine flow configurations both during plug generation and propagation events. More importantly, we demonstrate that exogenous surfactants provide protective coating films on airway walls and reduce flow instability-induced airway closure.

Experimental

Fabrication of the microfluidic device

The microfluidic device consisted of two poly(dimethylsiloxane) (PDMS) chambers separated by a porous polyester membrane of 3 μm pore size, which mimics the basement membrane in vivo (Fig. 1b). The dimensions of top and bottom microchannels were 350 μm × 85 μm and 550 μm × 85 μm, respectively. Both layers were fabricated using soft lithography.[29] Prepolymer (Sylgard 184, Dow-Corning) at a 1:10 curing agent-to-base ratio was cast against positive relief features to form negative replica of microchannels. The relief features were composed of SU-8 (MicroChem, Newton, MA) and fabricated on a thin silicon wafer using conventional photolithography. The prepolymer was cured at 60°C overnight. After cutting out the channel features, via holes to microchannels were punched using a 1.5 mm Biopsy punch (Miltex).

We used a stamping method to assemble the two PDMS layers and the porous membrane.[30] PDMS prepolymer was diluted 1:2 in toluene and spin-coated at 1000 rpm for 1 min on a glass

slide to form a thin layer of PDMS glue. Top and bottom layers of the device were stamped against the glue. The porous membrane was carefully placed on the bottom layer microchannel and small amounts of the glue were applied to the edges of the membrane using a pipette tip. Then, the two layers were carefully aligned under a microscope and the assembly was left at ambient temperature for ~1 h to degas. The device was cured at 60°C overnight. Finally, 14-gauge bent blunt needles (Becton Dickinson) were attached to silicone tubing (Fisher Scientific) of 10–15 cm and connected to inlet and outlet ports of air and liquid on the device using epoxy glue (ITW Performance Polymers). The fabrication procedure ensures a robust leakage-free bonding.

Wettability of microchannels

PDMS is intrinsically a hydrophobic material. To change the wetting properties of microchannels, we exposed devices to radiofrequency oxygen plasma (SPI Supplies) for time periods of 15, 20, and 25 min.[31] Plasma treatment was performed after attaching all tubings to microfluidic devices. To verify uniformity of plasma treatment along the length of the droplet observation region of microchannels, we estimated contact angles of liquid plugs in these devices and found that increasing duration of plasma treatment changed the contact angle from ~83° to ~73° to ~65°, respectively. Contact angles were estimated by extracting the profile of liquid plugs from experimental images using a freeware program, ImageJ (NIH), and subsequently fitting a tangent to the extracted profile at the point of contact with the channel wall.

Working fluids and viscosity and surface tension measurements

We selected three different working fluids: (i) Dulbecco's Phosphate Buffered Saline (PBS, Gibco), (ii) a 5 mM Tween 20 (Sigma) surfactant solution in PBS, and (iii) a natural lung surfactant, Survanta, with a concentration of 1.0 mg/ml in PBS. Liquid viscosity was measured using a U-tube viscometer (Ostwald). Surface tension of liquids was determined by Du Noüy ring method (Krüss).

Experimental setup design

The experimental setup of the plug generator is shown in Fig. 1c. In all experiments, liquid flow rate was fixed at 10 ml/hr and the source pressure of the air was adjusted to 10 psi using a pressure regulator on the air tank. An air flow meter (Cole-Parmer) installed upstream of the air inlet port of the microfluidic device significantly reduced the pressure of air supplied to the device. To generate liquid plugs on-chip, liquid was pumped into the K-shaped top microchannel using a syringe pump (KD Scientific) and was focused by compressed air stream to form a stratified air-liquid flow where the two streams flow side-by-side (Fig. 2a-1). Using a programmable solenoid pinch valve (Cole-Parmer) to close tubing connecting air source to the plug generator, the airflow was blocked for a very short predefined period of time ($\geq$30 ms), allowing the liquid to spread and progress towards the main channel (Fig. 2a-2). Recovery of the airflow re-established the stratified flow and pinched off a liquid plug that propagated downstream the main channel (Fig. 2a–3). To gain precise control over liquid plug dynamics and to mimic physiologic airway pressures, we used a sensitive pressure controlling mechanism that consisted of a small piece of plastic tubing glued to a 1 ml pipette tip at one end and placed between tunable squeeze jaws at the other end (Fig. 1c). This assembly was connected to the tubing at the outlet of the top chamber. A differential pressure transducer (Omega Engineering) was incorporated in the system to monitor the pressure difference, ΔP, between the inlet port of the air stream (P_1) and the outlet port of the top channel (P_2). Any change in air and liquid flow rates or fine tuning the closure of the squeeze jaws changed pressure within the system. The transducer translated this differential pressure into an electric voltage, which was measured

using a data acquisition (DAQ) board. The voltage data were converted to pressure data using manufacturer's tables.

Data analysis

The device was placed under a conventional bright field microscope (TS100, Nikon) during the experiment. Images and videos were captured using a Hamamatsu camera (Orca-ER) mounted on the microscope. ImageJ was used to analyze the images.

Results and discussion

For a liquid of known physical properties, we identified two main parameters that affect the plug generation process (assuming fixed channel dimensions and a constant liquid flow rate): differential pressure between the air inlet and the outlet port downstream of the main channel and wettability of the channel walls. These are discussed in the next two sections. Additionally, liquid surface tension is an important parameter in lung physiology. We use PBS and Survanta as working fluids to examine this point in the context of plug generation and propagation events in two separate sections following. Finally we discuss clinical implications of the findings.

Differential pressure

The baseline value of the differential pressure, ΔP, was adjusted by varying the airflow rate, the liquid flow rate, or the closure time of the pinch valve while keeping the closure of the squeeze jaws of the pressure controlling mechanism fixed. By varying the airflow rate, a large range of pressures including both physiologic transpulmonary pressures (ΔP<~0.5psi)[32] and abnormally larger non-physiologic pressures33 were accommodated in the microfluidic airway model (supporting information, Fig. SI.1a). We found that ΔP was hardly sensitive to changes in the liquid flow rate (supporting information, Fig. SI.1b) and therefore kept the liquid flow rate constant in all experiments and varied ΔP by changing the airflow rate. To examine pressure changes in the channel during generation and propagation of a liquid plug, we analyzed a typical pressure profile. Initially when both air and liquid flow at constant rates of 35 cm^3/min and 0.167cm^3/min, respectively, to form a stratified flow, ΔP has a constant baseline value of ~0.3 psi (region A in Fig. 2b corresponding to Fig. 2a-1). Closing off the pinch valve for 30 ms blocks the airflow momentarily, causing air pressure to build up behind the pinch valve due to the flow of air upstream of the pinch valve. The differential pressure rises sharply and reaches a peak value, ΔP_{peak}, about 50% larger than the baseline value in this case (region B in Fig. 2b). Once the pinch valve is reopened, the air pressure pushes the liquid column of the side channel toward the waste reservoir and the main channel. The stratified flow is recovered and a plug forms in the main channel (Fig. 2a-3). The pressure drops considerably, yet to a value larger than the baseline pressure (region C in Fig. 2b). This difference reflects resistance to the airflow in the main channel due to the presence of the liquid plug and indicates that in vivo, occluded lung airways that exist at the beginning of the inspiration cycle require a larger pressure to expand, causing small lung compliance.[32] The pressure remains at this level as the plug propagates downstream the channel and finally returns back to its baseline value after the plug is cleared from the channel (region D in Fig. 2b). This situation resembles increase in the lung compliance after collapsed lung units are reinflated (recruitment).

Reopening of the pinch valve is the onset of the plug generation process when the maximum inlet air pressure, and hence ΔP_{peak}, directly affects the flow at the K-junction of the device by pushing the liquid column (Fig. 2a-2) towards the main channel and the waste reservoir. Due to its larger resistance, the main channel is filled with less liquid compared to the channel leading to the waste reservoir. It will be shown below that at a constant liquid flow rate, ΔP_{peak} directly correlates with the size of liquid plugs (see Fig. 4). The increase in the liquid plug size with ΔP_{peak} is due to the ease of reinitiating flow into the air-filled main channel

compared to the liquid-filled side channel. We obtained a wide range of ΔP_{peak} by (i) changing the baseline air pressure and (ii) duration of closure of the pinch valve (supporting information, Fig. SI.2a).

Surface wettability of microchannels

Because of the large surface area-to-volume ratios, surface wettability is a critical parameter in microscale air-liquid two-phase flows. That is, one cannot simply control ΔP_{peak} and fluid flow rates and expect the same plug size in microchannels of differing wettabilities. We thus evaluated the role of wettability of microchannel surfaces using two sets of identical devices with different wettabilities: A microfluidic device that was rendered hydrophilic by exposure to oxygen plasma for 25 min and a hydrophobic device without any plasma treatment. To verify differences in surface properties, a PBS plug was formed in each device and advanced slowly using an extremely low airflow to ensure that the front meniscus attains an advancing contact angle.[34] Plugs generated in the plasma treated device yielded a much smaller contact angle, confirming hydrophilicity of channel surfaces (cf. Fig. 3a&3b). Next we performed plug generation experiments with hydrophobic and hydrophilic devices using similar air and liquid flow rates and the pinch valve closure time. As shown in Fig. 3c&3d, larger plugs are generated in the hydrophilic device compared to the hydrophobic one under similar test conditions. We calculated the solid-liquid interfacial tension (γ_{sl}) in these two systems to explain this observation:

The surface tension of PBS is similar to that of water at room temperature, γ_{lv}= 72.2 mJ/m^2, and therefore a similar contact angle (θ) is resulted on hydrophobic PDMS, i.e. ~105° (Fig. 3a).[35] We also estimated that PBS contact angle on hydrophilic PDMS surface is ~65° (Fig. 3b). To calculate γ_{sl}, first we invoke Young's equation

$$\gamma_{lv}\cos\theta=\gamma_{sv}-\gamma_{sl} \tag{1}$$

and an equation of state for interfacial tensions

$$\gamma_{sl}=\gamma_{lv}+\gamma_{sv}-2\sqrt{\gamma_{lv}\gamma_{sv}}\ e^{-\beta(\gamma_{lv}-\gamma_{sv})^2} \tag{2}$$

In Eq. (2), γ_{lv}, γ_{sv}, and γ_{sl} represent liquid surface tension, solid surface tension, and solid-liquid interfacial tension, respectively, and β=0.000125 (mJ/m^2)$^{-2}$ is an experimental constant.[36, 37]

Combining the above equations gives

$$\cos\theta=-1+2\sqrt{\frac{\gamma_{sv}}{\gamma_{lv}}}\ e^{-\beta(\gamma_{lv}-\gamma_{sv})^2} \tag{3}$$

Using known values of γ_{lv} and θ, Eq. (3) is used to first calculate γ_{sv} for both systems: $\gamma_{sv,\ hydrophobic}$=19.8 mJ/m^2 and $\gamma_{sv,\ hydrophilic}$=44.0 mJ/m^2. Subsequently, Young's equation is solved for γ_{sl} using γ_{sv}, γ_{lv}, and θ values of each system. This yields $\gamma_{sl,\ hydrophobic}$=38.5 mJ/m^2 and $\gamma_{sl,\ hydrophilic}$=13.6 mJ/m^2.

This analysis shows that the solid-liquid interfacial tension, which is the energy required to create a unit area of solid-liquid interface, is significantly larger for the hydrophobic system.

Therefore under similar test conditions, the hydrophobic device results in a smaller solid-liquid contact area (i.e., a shorter plug).

Quantification of plug generation with PBS and surfactant solutions at different surface wettabilities and peak differential pressures (ΔP_{peak})

We first used PBS as the working fluid to study plug generation in three sets of microfluidic devices with different channel wall surface tensions (γ_{sv}) of 33.2, 39.4, and 44.0 mJ/m^2, obtained by oxygen plasma treatment for 15, 20, and 25 min, respectively. The experiments were performed in a wide range of peak differential pressure, ΔP_{peak}<1.0 psi. These conditions enabled us to study simultaneously the combined effect of surface wettability and ΔP_{peak} on plug generation. We found a critical pressure (ΔP_c~0.22 psi) below which PBS plugs do not form; but rather, small droplets of large curvature are deposited on the channel walls. At $\Delta P_{peak} \geq \Delta P_c$, sufficient volume of PBS entered into the main channel to generate a plug across channel walls. Above the critical pressure level, in all three devices, the plug size initially increased linearly with the peak differential pressure up to a certain pressure threshold (Fig. 4a). At a given pressure, larger plugs form in more hydrophilic channels (larger slope for diamonds than squares and triangles in Fig. 4a) due to a smaller solid-liquid interfacial tension, γ_{sl}, in these systems, as explained above and corroborated by non-dimensionalizing the peak differential pressure with respect to γ_{sl} that results in the collapse of all three series of data points toward a linear band (supporting information, Fig. SI.3).

At a certain pressure threshold, further increase of ΔP_{peak} does not yield larger plugs, but rather multiple plugs are generated (Fig. 4b). To understand this phenomenon, we performed video imaging of the process. As pressure increases, instabilities of the two-phase flow during reopening of the air stream leave small liquid residues on channel walls, in addition to the generated liquid plug. At pressures below the threshold value, the residues are small and remain immobile under the airflow. However higher air pressures generate larger residues that move toward the entrance of the main channel and merge to form a second and even a third plug (Fig. 4b& a video in the supporting information).

We also evaluated the plug generation process by varying ΔP_{peak} using different valve closure times. The size of PBS plugs continuously increased with ΔP_{peak} up to ~0.45 psi that corresponds to a valve closure time of ~500 ms (Fig. SI.2b). Thereafter, the plug size only changed marginally because at valve closure times greater than 500 ms, increase in the peak pressure significantly slows down (Fig. SI.2a).

Surfactant is a critical component of the respiratory system for normal function of the lung. During clinical events such as SRT, surfactant plugs can form in upper airways. To evaluate formation of pulmonary surfactant plugs, we used Survanta as the working fluid. Survanta, a clinical exogeneous surfactant, is an extract of minced bovine lung tissue to which certain components are added to mimic surface tension-lowering properties of natural lung surfactant.[38] We used a hydrophilic device with γ_{sv}=44.0 mJ/m^2 in a pressure range similar to the PBS tests, i.e. ΔP_{peak}<1.0 psi. This surface wettability condition was selected because it more closely mimics hydrophilic airways in vivo. Similar to PBS, Survanta plugs do not form below a critical pressure level. However, this minimum is larger for Survanta (ΔP_c~0.29 psi). We observed that unlike PBS, Survanta always tends to spread on channel walls rather than forming fairly round droplets. Therefore it takes a larger pressure and a greater volume of liquid to generate a Survanta plug. This delayed plug formation is mediated by the low surface tension of Survanta ($\gamma_{Survanta}$= 25.0 mJ/m^2 vs. γ_{PBS}= 72.2 mJ/m^2) and a resulting low γ_{sl} and supports a protective role of surfactant against airway closure due to flow instabilities. Above the critical pressure, the plug length increases linearly with pressure up to ~0.65 psi (Fig. 4a,c). Under similar pressure and wettability conditions, Survanta plugs are always shorter than PBS plugs (c.f. circles and diamonds in Fig. 4a) because a significant volume of Survanta entering into

the main channel spreads on the walls behind the plug. As pressure increases to ΔP_{peak}>0.65 psi, Survanta deposition becomes even more significant and the plug size remains fairly constant (Fig. 4a,c). Spreading of Survanta is also the key factor preventing multiple plug formation, as opposed to the surfactant-free PBS solution.

Propagation of PBS and surfactant solution liquid plugs

Subsequent to the formation of liquid plugs, the inspired air pressure drives the plug along the airway. Understanding this process in detail and the ability to systematically manipulate it is important to events such as plug-mediated airway injury and SRT. Questions that have largely been studied numerically and yet require experimental analysis are differences in the propagation dynamics of buffer and surfactant solution plugs under similar channel wettability and driving pressure,[13, 39, 40] conditions mediating rupture of liquid plugs,[15] and correlation between plug size and speed.[15]

We tested both PBS and a 5 mM solution of Tween 20 as a model surfactant in hydrophilic microfluidic devices. A key observation was that unlike PBS plugs, the rear meniscus of model surfactant plugs deposited a thin film on channel walls (cf. Fig. 5a and 5b) and the plug length decreased approximately 60% over a distance of ~6.7 mm. We monitored the displacement of front meniscus (X_{front}) and rear meniscus (X_{rear}) of the surfactant plug from an origin point in the main channel where plug propagation starts. The displacement of both menisci followed quadratic polynomial relations and the data suggested that the rear meniscus propagated slightly faster than the front one (Fig. 5c). This experiment is consistent with a previous observation[28] and suggests that plug rupture is due to a faster rear meniscus eventually catching up with the front one. Equating the displacement equations gave the time of the surfactant plug rupture in the channel, t=36.45 sec. Using this value, the site of plug rupture is estimated from the displacement equations to be ~10.9 mm downstream the origin point. This estimate is valid for a straight homogeneous channel only. Our microfluidic setting contains a porous membrane downstream the channel allowing liquid to purge through the membrane, complicating dynamics of plug propagation/rupture. Nevertheless, in the presence of a monolayer of differentiated epithelial cells on the membrane, the channel can still be considered homogeneous because cell-secreted tight junctional proteins limit paracellular (passive) fluid transport and therefore, the above estimate should still remain valid (see supporting information, Fig. SI.4). Thus, this microfluidic platform enables generation of well-defined liquid plugs that can be ruptured at a pre-determined region over a cell monolayer to investigate the extent of damage to airway cells solely due to plug rupture and distinguish it from that caused by plug propagation.

The variation of surfactant plug length over time was deduced from differences between front and rear menisci displacements of Tween plugs. The result in Fig. 5d indicates that the plug length decreases non-linearly with time and the plug speeds up as it becomes shorter (circles). This observation indicates that under a constant driving air pressure, larger plugs propagate more slowly, most likely due to a stronger viscous resistance, consistent with a recent numerical investigation of unsteady propagation of liquid plugs in a straight tube.[15] Unlike Surfactant-containing plugs, PBS plugs did not deposit a detectable trailing film (diamonds). Interestingly, we also found that the propagation of surfactant plugs is associated with the formation of a precursor film that moves ahead of the contact line of the front meniscus of the plug on the microchannel surface (Fig. 5e& a video in the supporting information). The precursor film formation is likely due to interactions between surfactant head groups and the hydrophilic surface of the channel.[41]

Propagation speed of liquid plugs is another key parameter that influences both the outcome of SRT and airways cell injury due to pathological liquid plugs. To demonstrate the utility of our in vitro platform for such studies, we examined PBS and 5 mM Tween 20 surfactant plug

propagation at different speeds realized by tuning the pressure of driving air while keeping other parameters fixed. Under a constant driving air pressure and assuming steady plug propagation, plug speed was obtained by dividing plug displacement over a certain distance with the propagation time. The results in Fig, 6 show that PBS plugs propagated about 2.5 times faster than surfactant plugs under similar driving pressures, consistent with computational data.[40] Increasing the driving pressure from ~0.15 psi to 0.32 psi changes the speed of PBS plugs from 1.9 mm/sec to 5.3 mm/sec whereas the speed of surfactant plugs increases from 0.7 mm/sec to 2.2 mm/sec. The capillary number in these experiments is on the order of 10^{-5}, showing that the flow is surface tension dominant.

We note that the described platform allowed us to experimentally study fundamental liquid plug dynamics that, until now, have been primarily the realm of computational analysis. Our experimental data verified computational findings about differences in propagation dynamics of buffer and surfactant solution plugs in terms of trailing and precursor film deposition and plug speed under similar test conditions, as well as correlation between size and speed of liquid plugs and non-linear increase in plug speed with increase in driving air pressure.[40]

Clinical implications

Flow instabilities under large air pressures (~>0.5 psi) led to the formation of PBS drops (residues) of high curvature on channel walls that resulted in multiple occluding liquid plugs (see the movie in the supporting information). This experiment cautions the use of large ventilation pressures in patients with surfactant deficiency.[42] The fact that PBS plugs propagated along the length of the channel without forming trailing or precursor films on the channel walls reinforces this consideration. This is because the largest mechanical forces on airway walls due to plug propagation are always generated at thin front and rear menisci,[13] and such abnormal forces may cause significant damage to airway cells.

We showed that unlike PBS, Survanta plug formation required a larger pressure. Furthermore under flow instabilities at high air pressures (~0.5–0.9 psi), 1.0 mg/ml physiologic surfactant prevented formation of trailing plugs; rather, Survanta always spread on the channel walls. This is consistent with earlier bench-top experiments and computational models that suggested a stabilizing effect for surfactant delaying meniscus formation in rigid airway models by a factor of 4–5 compared to surfactant-free solutions.[4, 43, 44] Thus, the clinical benefits of providing exogenous surfactant to patients is in part for maintaining airway patency and protecting the epithelial lining cells from the damaging forces of repetitive opening and closing.

Propagation of surfactant plugs was also quite different from PBS plugs and was always accompanied by formation of a trailing film due to deposition onto channel walls and a precursor film moving ahead of the plug. Measurements of viscosity and surface tension of PBS and Tween 20 helped explain the difference. Both liquids have a low viscosity (μ_{PBS}=1.00 cP and μ_{Tween}=1.07 cP) whereas the 5 mM Tween 20 solution has a significantly lower surface tension (γ_{Tween}=37.4 mJ/m^2) compared to PBS (γ_{PBS}=72.2 mJ/m^2). This indicates that formation of surfactant films on hydrophilic channel walls is mediated by a low surface tension, which most likely is due to adsorption of surface-active molecules at the air-liquid interface of the surfactant plug. This is consistent with findings from numerical models that suggest decrease in the surface tension of the working fluid correlates with increase in the film thickness.[15] Presence of precursor and trailing surfactant films is thought to protect airway cells against mechanical stresses of non-physiologic flows. Indeed, numerical models show that surfactant mitigates mechanical forces (pressure, shear stress, and their gradients) on airway walls and the peak value of these forces decrease as the film thickness increases.[16, 40]

Airways are accessible paths for the delivery of genetic materials and drug molecules to treat genetic lung diseases such as cystic fibrosis and arrest the progression of lung cancer. Surfactant

liquid plugs are considered potential drug delivery vehicles in the lung. However, the success of such treatments will greatly depend on the accuracy of targeted delivery of liquid plugs to airways.[45] Based on a moderate driving pressure of ~0.3 psi in this in vitro model, we showed that the site of rupture of surfactant plugs can be estimated from plug displacement equations. Our approach and automated platform will facilitate studies of targeted drug and gene delivery to pre-determined regions of the lung airway tree.

Another key observation relevant to SRT in clinics was that increasing the driving air pressure caused faster propagation of surfactant plugs and resulted in the rupture of the plug earlier in the channel due to a more significant deposition onto channel walls (note: trailing film thickness is proportional to plug speed).[5] This highlights the importance of delivery of exogenous surfactant to patients at moderate pressures to prevent premature rupture of surfactant plug and incomplete delivery, validating predictions from existing computational data.39 Thus, our approach may be utilized to define optimum conditions for SRT to ensure that sufficient volume of surfactant reaches conducting airways to allow uniform surfactant distribution on airway walls.

Conclusions

We presented a micro-engineering approach to model the architecture of pulmonary airways and study associated liquid plug flows. Using computer-controlled mechanical components, liquid plugs of buffer and surfactant solutions with user-defined size and propagation speed were generated. We correlated formation and propagation of liquid plugs with physical properties of working liquids, wettability of channel walls, and pressure of the air stream. A minimum critical pressure was required to initiate plug generation and this minimum was larger when surfactant was added to PBS. For a fixed surface wettability, increasing the baseline pressure, and hence the peak differential pressure, generated larger PBS plugs up to a certain pressure threshold; thereafter, multiple liquid plugs formed due to increased flow instabilities. A physiologic surfactant solution, Survanta, behaved quite differently from PBS. The plug size initially increased with pressure but further increases in pressure, which caused larger flow instabilities, did not lead to the formation of additional trailing plugs. The addition of Survanta in hydrophilic channels mimics normal lung airways and these results suggest a critical role for pulmonary surfactant in maintaining airway patency. In contrast to PBS alone, propagating surfactant plugs gave rise to trailing and precursor films. Such surfactant coatings on airway walls may serve to protect airway tissue against mechanical stresses associated with non-physiologic flow conditions. Generation of well-defined surfactant-containing plugs in an in vitro platform is a new capability that will serve various studies in pulmonary research involving surfactants.

Our microfluidic airway model is a flexible in vitro platform that accommodates quantitative investigations of liquid plug dynamics by independently varying components that comprise the air-liquid interface in the lung. The findings and the proposed platform will help design and perform in vitro tests to understand cellular level effects of liquid plugs in airways and the efficacy of preventive and treatment strategies, such as SRT, for various respiratory disorders.

Supplementary Material

Refer to Web version on PubMed Central for supplementary material.

Acknowledgments

This work was supported by the National Institute of Health (HL084370). H. Tavana acknowledges a postdoctoral fellowship from NSERC Canada (PDF-329449-2006).

References

1. Weibel ER, Gomez DM. Science 1962;137:577. [PubMed: 14005590]
2. Levitzky, MG. Pulmonary Physiology. 7. The McGraw-Hill Companies Inc; 2007.
3. Macklem PT. Am J Respir Crit Care Med 1998;157:S181. [PubMed: 9606316]
4. Cassidy KJ, Halpern D, Ressler BG, Grotberg JB. J Appl Physiol 1999;87:415. [PubMed: 10409603]
5. Grotberg JB. Annu Rev Biomed Eng 2001;3:421. [PubMed: 11447070]
6. Griese M, Birrer P, Demirsoy A. Eur Respir J 1997;10:1983. [PubMed: 9311489]
7. Gunasekara L, Schoel WM, Schürch S, Amrein MW. Biochim Biophys Acta 2008;1778:433. [PubMed: 18036553]
8. Hohlfeld JM. Respir Res 2002;3:4. [PubMed: 11806839]
9. Meyer KC, Sharma A, Brown R, Weatherly M, Moya FR, Lewandoski JR, Zimmerman J. Chest 2000;118:164. [PubMed: 10893374]
10. Wright SM, Hockey PM, Enhorning G, Strong P, Reid KBM, Holgate ST, Djukanovic R, Postle AD. J Appl Physiol 2000;89:1283. [PubMed: 11007560]
11. Tavana H, Huh D, Grotberg JB, Takayama S. Lab Medicine 2009;40:203.
12. Pelosi P, Rocco PRM. Crit Care 2007;11:114. [PubMed: 17328793]
13. Fujioka H, Grotberg JB. J Biomech Eng 2004;126:567. [PubMed: 15648809]
14. Bilek AM, Dee KC, Gaver DP III. J Appl Physiol 2003;94:770. [PubMed: 12433851]
15. Fujioka H, Takayama S, Grotberg JB. Phys Fluids 2008;20:062104.
16. Ghadiali SN, Gaver DP. J Appl Physiol 2000;88:493. [PubMed: 10658016]
17. Halpern D, Grotberg JB. J Fluid Mech 1992;244:615.
18. Corbet A, Bucciarelli R, Goldman S, Mammel M, Wold D, Long W. J Pediatr 1991;118:277. [PubMed: 1993961]
19. Jobe AH. N Engl J Med 1993;328:861. [PubMed: 8441430]
20. Yapicioglu H, Yildizdas D, Bayram I, Sertdemir Y, Yilmaz HL. Pulm Pharmacol Ther 2003;16:327. [PubMed: 14580923]
21. Chu EK, Whitehead T, Slutsky SA. Crit Care Med 2004;32:168. [PubMed: 14707576]
22. D'Angelo E, Pecchiari M, Baraggia P, Saetta M, Balestro E, Milic-Emili J. J Appl Physiol 2002;92:949. [PubMed: 11842025]
23. Dos Santos C, Slutsky A. J Appl Physiol 2000;89:1645. [PubMed: 11007607]
24. Espinosa FF, Kamm RD. J Appl Physiol 1998;85:266. [PubMed: 9655785]
25. Huh D, Fujioka H, Tung YC, Futai N, Paine R, Grotberg JB, Takayama S. Proc Natl Acad Sci USA 2007;104:18886. [PubMed: 18006663]
26. Cubaud T, Ho CM. Phys Fluids 2004;16:4575.
27. Gunther A, Jhunjhunwala M, Thalmann M, Schmidt MA, Jensen KF. Langmuir 2005;21:1547. [PubMed: 15697306]
28. Ody CP, Baroud CN, Langre Ed. J Colloid Interface Sci 2007;308:231. [PubMed: 17234204]
29. Duffy DC, McDonald JC, Schueller OJA, Whitesides GM. Anal Chem 1998;70:4974.
30. Chueh BH, Huh D, Kyrtsos CR, Houssin T, Futai N, Takayama S. Anal Chem 2007;79:3504. [PubMed: 17388566]
31. Bowden N, Huck WTS, Paul KE, Whitesides GM. Appl Phys Lett 1999;75:2557.
32. West, JB. Respiratory Physiology: The Essentials. 8. Lippincott Williams & Wilkins; Philadelphia: 2008.
33. Tsuno K, Miura K, Takeya M, Kolobow T, Morioka T. Am Rev Respir Dis 1991;143:1115. [PubMed: 2024823]
34. Tavana H, Neumann AW. Adv Colloid Interface Sci 2007;132:1. [PubMed: 17222380]
35. Ferguson GS, Chaudhury MK, Biebuyck HA, Whitesides GM. Macromol 1993;26:5870.
36. Li D, Neumann AW. J Colloid Interface Sci 1990;137:304.
37. Tavana H, Gitiafroz R, Hair ML, Neumann AW. J Adhes 2004;80:705.
38. Willson DF, Chess PR, Notter RH. Pediatr Clin N Am 2008;55:545.

39. Waters SL, Grotberg JB. Phys Fluids 2002;14:471.
40. Fujioka H, Grotberg JB. Phys Fluids 2005;17:082102.
41. Frank B, Garoff S. Langmuir 1995;11:4333.
42. Dreyfuss D, Martin-Lefevre L, Saumon G. Respir Crit Care Med 1999;159:1752.
43. Halpern D, Grotberg JB. J Biomech Eng 1993;115:271. [PubMed: 8231142]
44. Otis DR, Johnson M, Pedley TJ, Kamm RD. J Appl Physiol 1993;75:1323. [PubMed: 8226547]
45. Halpern D, Fujioka H, Takayama S, Grotberg JB. Respir Physiol Neurobiol 2008;163:222. [PubMed: 18585985]

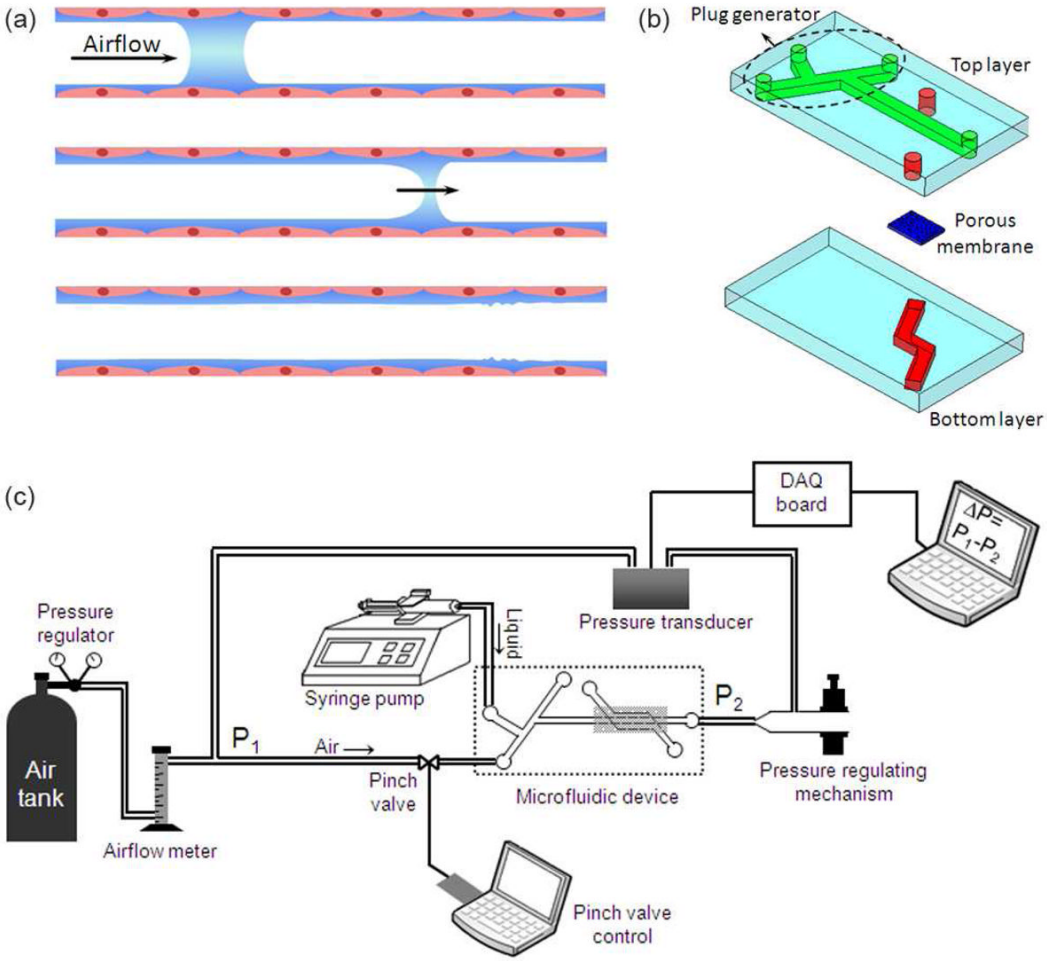

Fig. 1.

(a) Schematic of the obstruction of surfactant-deficient airways by liquid plugs. The plug moves downstream the airway due to the inhaled air pressure and eventually ruptures, (b) schematic of the two-layer microfluidic device, (c) schematic of the computerized liquid plug generating experimental setup.

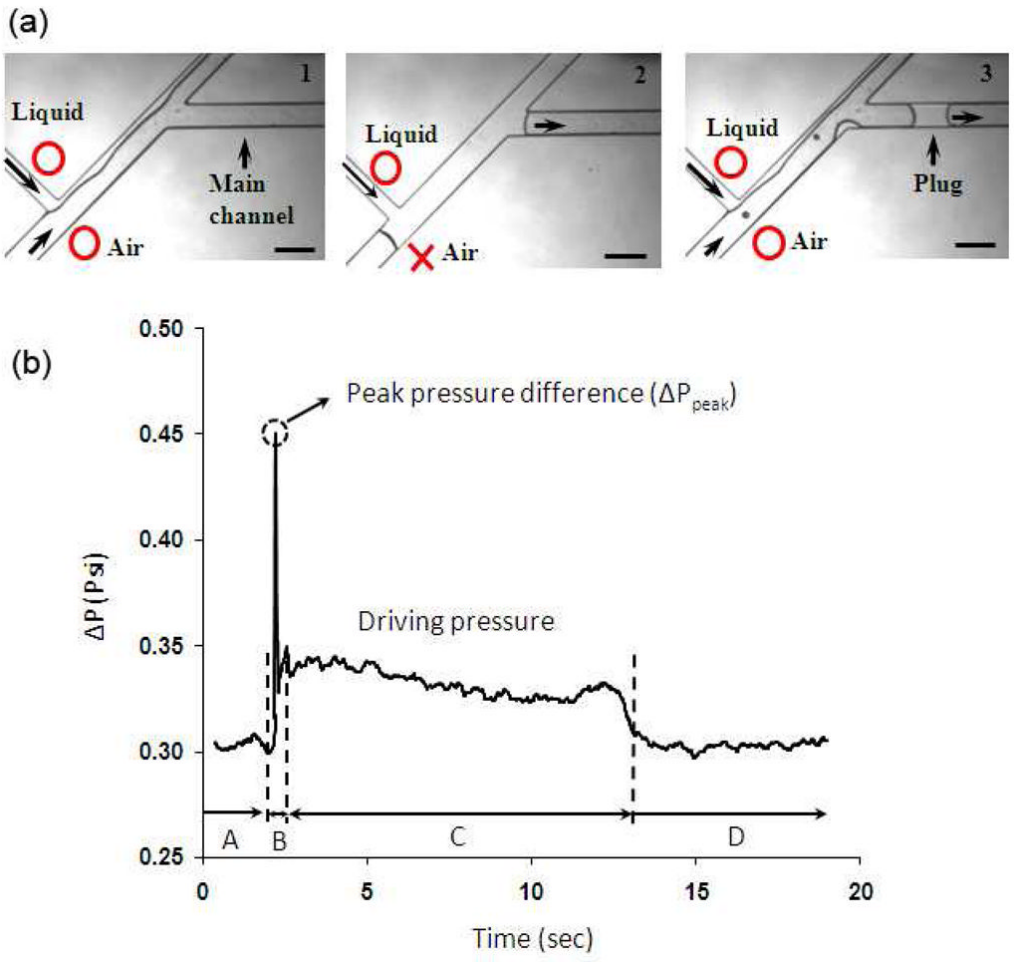

Fig. 2.

(a) Sequence of events during formation of liquid plugs. Open circle and cross symbols denote open and closed states of flows, (b) a typical pressure profile in the course of one plug generation/propagation event, scale bar 350 μm in a.

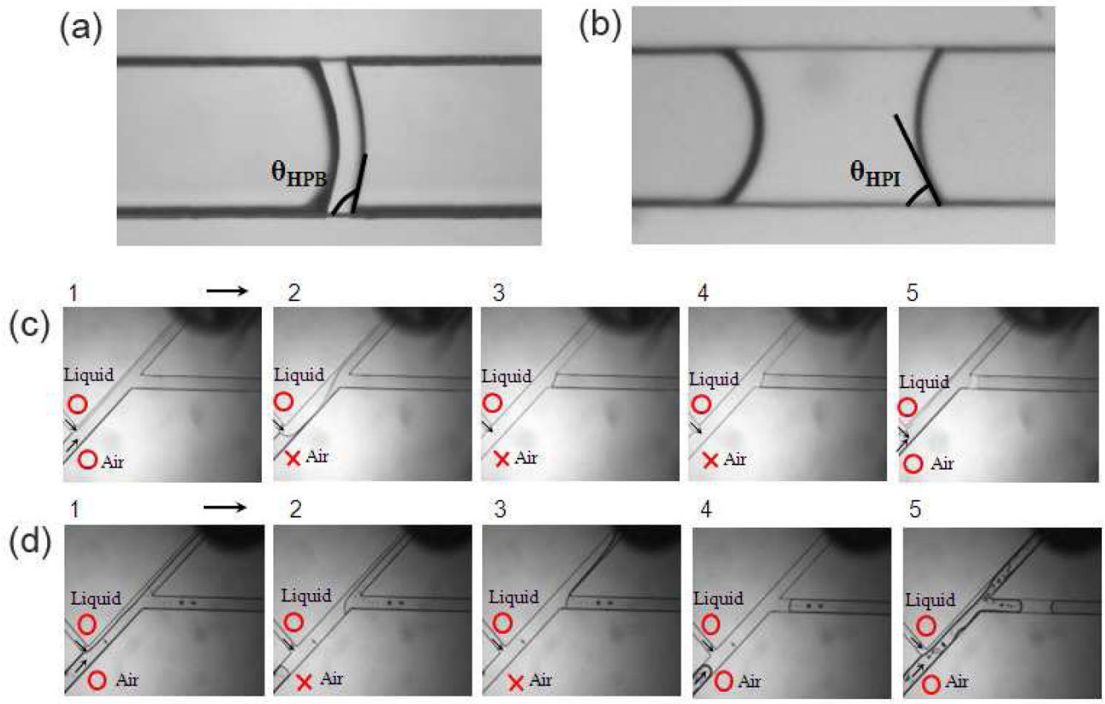

Fig. 3.

Advancing contact angles of PBS plugs in (a) hydrophobic and (b) hydrophilic PDMS microchannels, respectively. Plug generation in (c) hydrophobic and (d) hydrophilic microchannels, respectively, under similar test conditions.

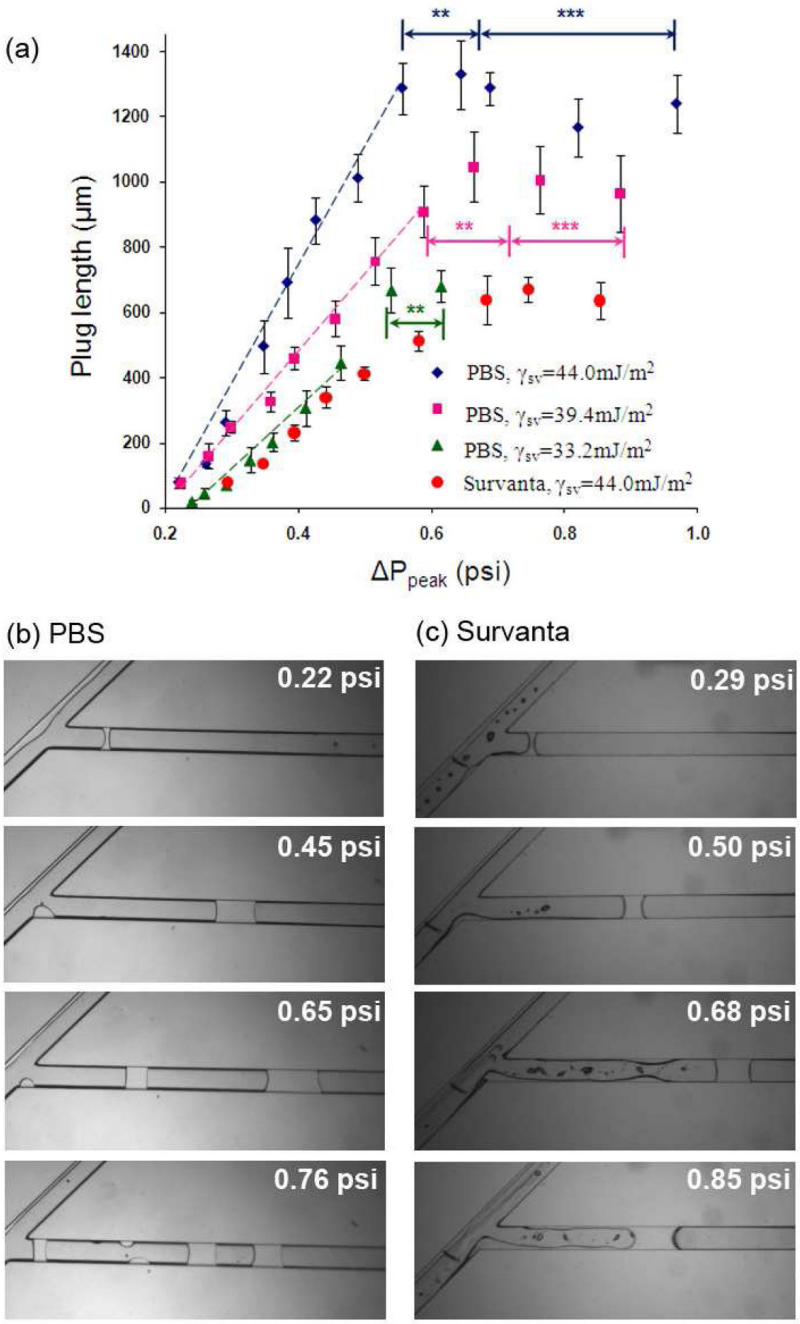

Fig. 4.

(a) Influence of channel surface wettability and peak differential pressure on the length of liquids plugs of PBS (diamonds, squares, and triangles) and Survanta (circles), (b) continuous increase in pressure causes formation of double and triple PBS plugs (noted by asterisks), (c) flow instabilities at similar pressure conditions do not generate trailing Survanta plugs.

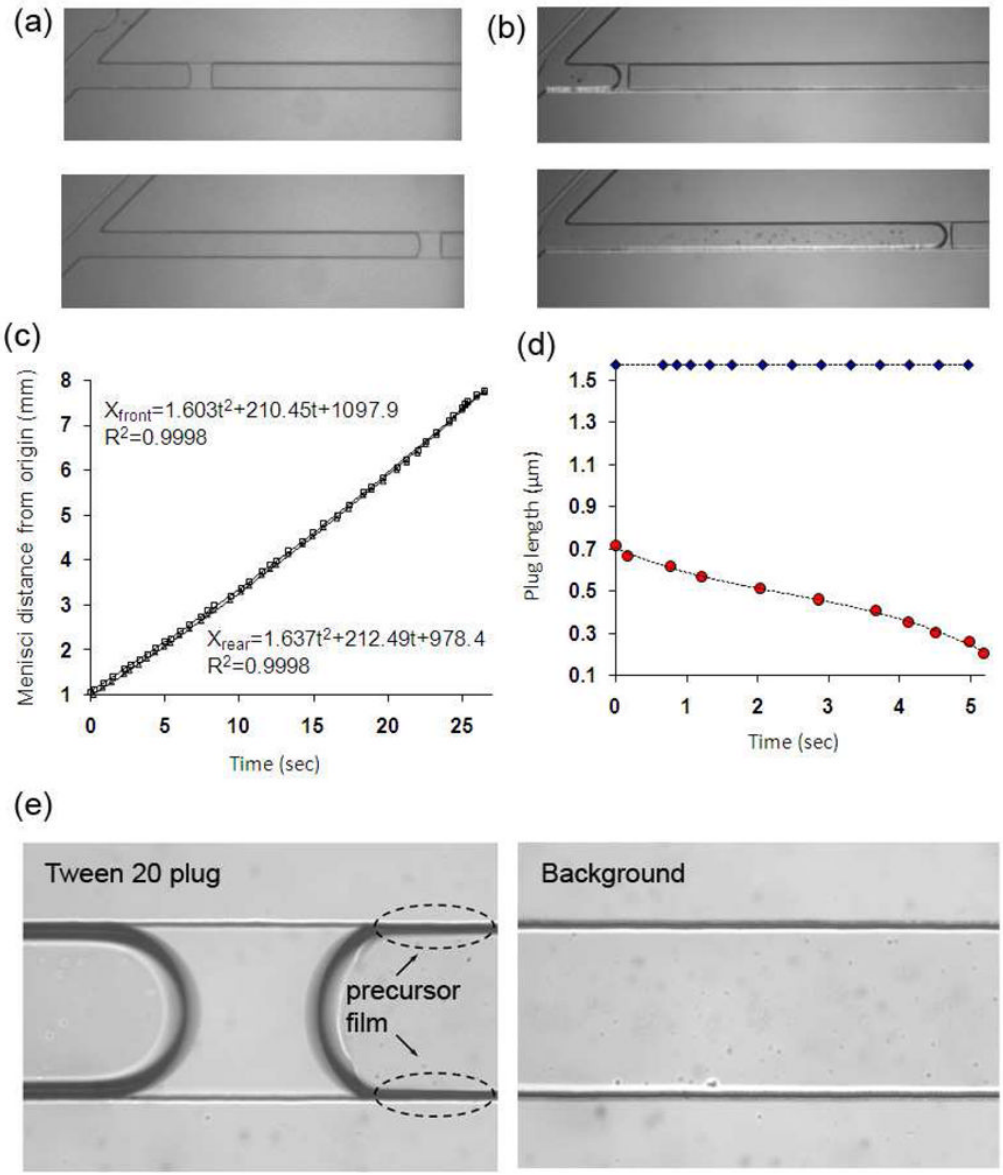

Fig. 5.

(a) PBS plugs propagate without detectable deposition onto channel walls whereas (b) surfactant-containing plugs deposit a thin trailing film, (c) displacement of front and rear menisci of the surfactant plug in (b), (d) variation of PBS (diamonds) and surfactant (circles) plug length due to deposit on channel walls, (e) a precursor film forms ahead of contact line of front meniscus of the propagating surfactant-containing plug (compare to the background channel image).

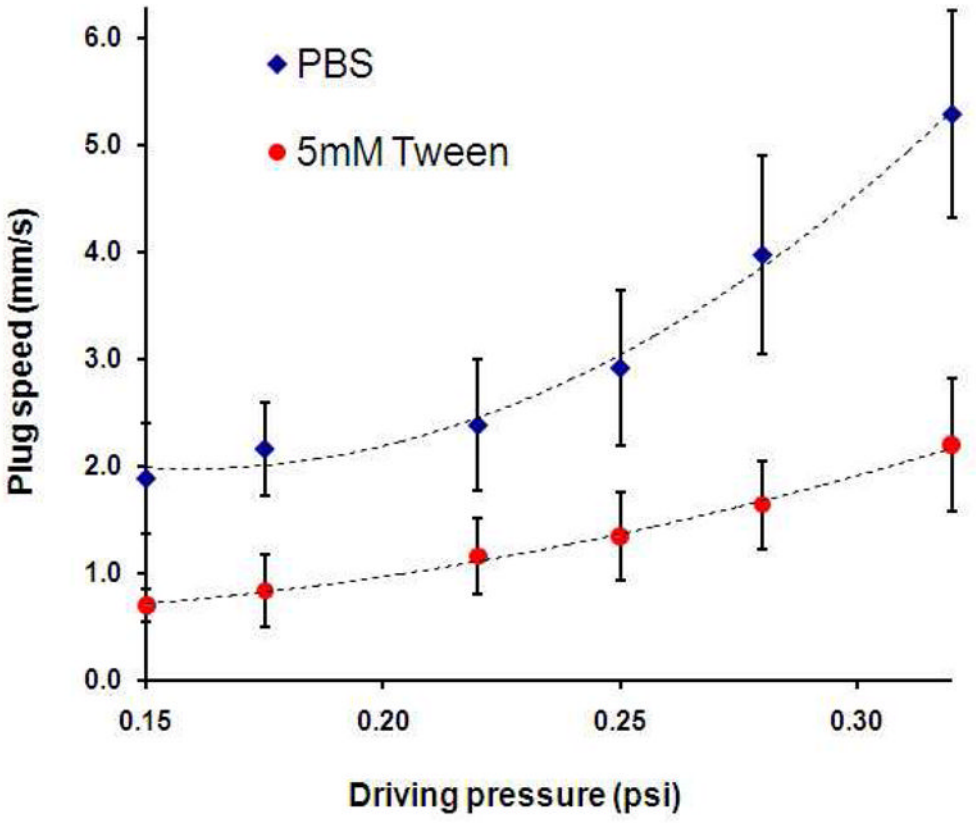

Fig. 6.

Propagation speed of PBS and surfactant liquid plugs is shown as a function of driving air pressure. Overall, PBS plugs propagate about 2.5 times faster than surfactant-containing plugs.